EARTH'S CRYOSPHERE
SCIENTIFIC JOURNAL

Earth's Cryosphere, 2022, vol. XXVI, No. 1, pp. 40–46 http://earthcryosphere.ru/

CRYOGENIC PHENOMENA IN SEAS AND OCEANS

ANALYSIS OF SHORT-RANGE SPATIAL AND TEMPORAL RELATIONSHIPS IN THE ICE DATA SET FOR THE NORTHERN HEMISPHERE

V.M. Fedorov, D.M. Frolov

Lomonosov Moscow State University, Faculty of Geography,
Leninskie Gory 1, Moscow, 119991 Russia; fedorov.msu@mail.ru, denisfrolovm@mail.ru

Autocorrelation characteristics of long-term time series of cells with the size of 1° × 1° of the sea ice area data array for the Northern Hemisphere are obtained. The temporal heterogeneity and spatial anisotropy in long-term variability of the sea ice area in the Northern Hemisphere are determined. The closest relationships between long-term monthly values of the sea ice area are typical for summer months. More than 49 % of maximum values of pair correlation coefficient are due to the connection of June and July, as well as July and August multiyear series in the array cells. This effect is a consequence of intense and massive summer melting of sea ice in the Northern Hemisphere and similarity of their long-term variability. The closest relationships in the neighboring cells of the array between the long-term monthly values of the sea ice area in all months of the year are noted for the east–west latitudinal direction. It accounts for more than 87 % of all maximum values of correlation coefficient. Spatial anisotropy is revealed throughout the entire area to the north of the Arctic Circle. The reason for this effect is determined by the features of sea ice seasonal formation (mainly from high latitudes to low latitudes) and melting (from low latitudes to high latitudes). These features are associated with seasonal changes in insolation. Long-term changes in sea ice area have similar direction and are determined by changes in meridional gradient of insolation. Another reason may be mainly meridional direction of sea ice drift in the Arctic Ocean. Areas with high and low levels of short-range spatial and temporal relationships in sea ice area dynamics in the Northern Hemisphere are determined.

Keywords: *sea ice area, Northern Hemisphere, dynamics, spatial and temporal relationships, spatial heterogeneity, spatial anisotropy*

INTRODUCTION

A highly important parameter of the ice cover is its area, which changes both in space and in time. The study of changes in the area of sea ice and the reasons leading to these changes is one of the most current goals of sea ice science [*Zakharov, 1976; Frolov and Gavrilo, 1997*]. The distribution of sea ice depends on many factors controlled by geophysical processes. First, these are air temperature and humidity, ocean surface temperature, circulation processes in the atmosphere, sea currents, halocline presence and structure, cloudiness, surface runoff, albedo, and others. The foundation of these factors is the solar radiation coming to Earth, the main energy source of hydrometeorological processes [*Shuleikin, 1953; Kondratiev, 1980, 1992; Monin, 1982*]. Irregularities in the entry of solar radiation over time and its uneven distribution in space are responsible for heat exchange processes – "a thermal machine of the first and second order" [*Shuleikin, 1953*]. Because of heterogeneity in the components of the environment, heat exchange between the atmosphere, ocean, and sea ice takes place. Sea ice represents a dynamic component of the environment, for which a seasonal, year-to-year, and long-term variability is typical. The goal of this work is to analyze short-range spatial and temporal relationships within the sea ice data set in order to determine patterns of long-term variability in the sea ice area.

The HadISST1 [*http://www.metoffice...*] data set, which contains data on sea surface temperature (SST) and sea ice area from the end of the 19th century to the present time, can serve as the foundation for research into modern climate and sea ice dynamics (climate indicators) with a high spatial and temporal resolution. This data set can also be used to produce more accurate sea ice distribution models. As such, the HadISST1 data set has a high scientific value. However, it clearly has disadvantages related to the absence of source data for certain regions and time periods and to the methods of data calculation, interpolation, and extrapolation [*Rayner et al., 2003*]. Thus, the determination of representative indicators (correlation characteristics) of short-range relationships for the clarification and correction of sea ice data is a highly relevant geophysical problem.

OBJECTS AND METHODS

The Hadley Centre sea ice and sea surface temperature data set (HadISST1) developed at the Met Office Hadley Centre for Climate Prediction and Research (UK) was used as the study object [*http://www.metoffice...*]. Information about monthly SST and sea ice area in the Northern and Southern hemi-

Copyright © 2022 V.M. Fedorov, D.M. Frolov, All rights reserved.

spheres in the HadISST1 database was obtained as a result of the integration of reanalysis data (ERA40) (completed using empirical orthogonal functions (EOF) and instrumental and visual observation data (firstly from ships and satellites)) into a single data set. Reconstruction of sea ice area in cells of size 1° × 1° was completed based on approximation algorithms and extrapolation of available data (digitized maps of sea ice area, observation data from ships and satellites) with consideration for sea surface temperature (SST) [*Rayner et al., 2003*].

The data set presents data on the monthly sea ice area averaged for grid cells of 1° × 1° in percent of the area of the cell (ice coverage) from 1870 to the present day. The authors analyzed the interval from 1978 to 2018 (the period of satellite observations) in the Northern Hemisphere. The considered data set includes almost 7400 grid cells in the Northern Hemisphere. Each cell presents information about ice coverage with monthly resolution.

The estimation and significance of the linear correlation coefficient during correlation analysis was determined in accordance with existing methods [*Zaks, 1976*]. The standard error of the correlation coefficient was calculated using the formula:

$$m_r = \sqrt{\frac{1-r^2}{n-2}},$$

where r is the sample correlation coefficient, and n is the sample size.

The statistical significance of the linear correlation coefficient was determined using Student's t-test, the factual value of which was calculated using the formula:

$$t_{\text{fact}} = \frac{|r|}{m_r}.$$

Conclusions about the significance of r are made based on the comparison of t_{fact} and t_{cr} (α, $n-2$) – critical (tabular) value of t-distribution, where α is the level of significance, and $(n-2)$ is the number of degrees of freedom. The correlation coefficient is considered statistically significant if $t_{\text{fact}} > t_{\text{cr}}$. In other cases, it is statistically insignificant.

RESULTS AND DISCUSSION

Analysis of temporal relationships. To determine temporal relationships, a correlation analysis of long-term monthly values of sea ice area was conducted. Correlations between long-term values (temporal series ranging from 1978 to 2018) of consecutive months in each cell were calculated. Thus, January values of sea ice area were correlated with February values, etc. December values of sea ice area were correlated with January values. The average value was found for each cell from correlation coefficients obtained using pair correlations for all 12 months of the year (Fig. 1).

Significant values of correlation coefficient (averaged for a month) were noted for the Barents and Greenland seas, the Davis Strait and the eastern part of the Sea of Okhotsk. The distribution of maximum values of the correlation coefficient was also analyzed (Fig. 2).

High values (>0.65) of the coefficient of pair correlation (for individual months) were noted for a larger part of the northern polar region. The closest ($R > 0.8$) correlation for individual months was manifested for the Greenland and Barents seas, East Siberian and Chukchi seas, the Beaufort Sea, the Hudson Strait, the Davis Strait, and the northern part of the Baffin Bay.

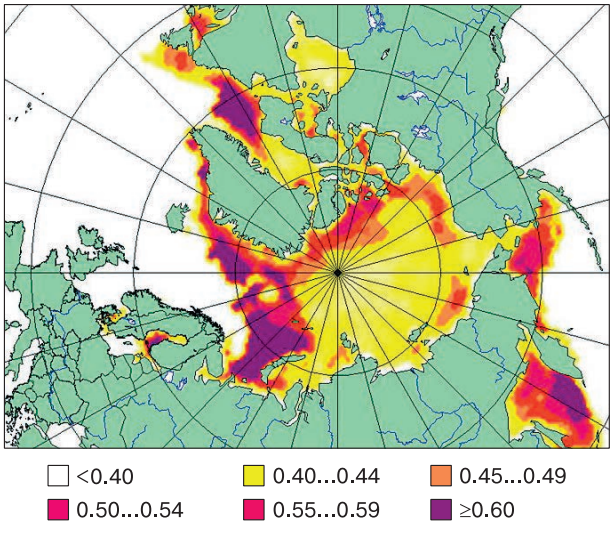

Fig. 1. Distribution of average values of the correlation coefficient.

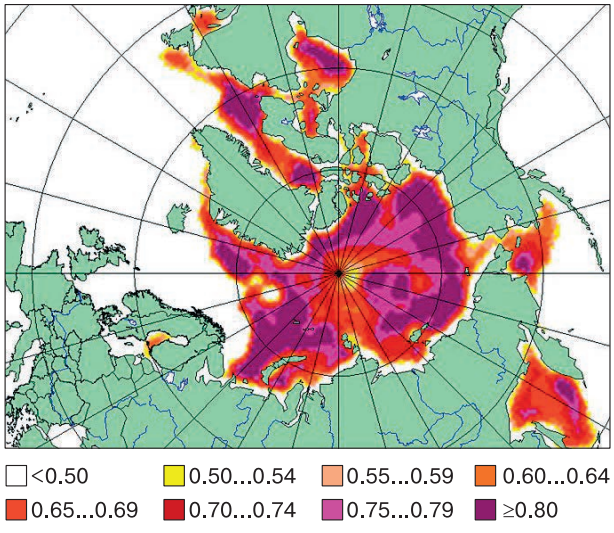

Fig. 2. Distribution of maximum values of the correlation coefficient.

Table 1. **Distribution of maximum correlation coefficients in pair correlations (%)**

Months	Correlation coefficient
January–February	3.567
February–March	1.953
March–April	5.775
April–May	4.352
May–June	5.843
June–July	34.650
July–August	14.374
August–September	6.879
September–October	9.023
October–November	7.282
November–December	2.272
December–January	6.030

Most of the high correlation coefficients were observed for the relationship between long-term series of June and July, as well as between July and August (Table 1). Thus, 49.024 % of high correlation coefficients fall on the summer season. The effect of a close relationship between sea ice area in adjacent cells in the summer is clearly a consequence of active sea ice melting determined by the maximum seasonal insolation [*Fedorov, 2018*] with a consecutive decrease in sea ice area from June to July and August. Thus, sea ice area in July is determined to a significant extent by sea ice area in June. The period of intense ice melting occurs during the summer solstice, when the seasonal maximum of heat influx from solar radiation is observed in the Northern Hemisphere. Earlier, the effect of the close relationship of ice coverage in the summer months on a sea scale was noted for the Barents [*Zakharov and Malinin, 2000*] and other seas of the Russian Arctic [*Frolov and Gavrilo, 1997; Zubakin, 2006; Fedorov, 2015; Fedorov et al., 2020*]. However, thus summer relationship is largely preserved in the northern polar region on a scale of 1° × 1° grid cells.

Thus, the analysis of temporal relationships in the HadISST1 ice data set indicates that maximum correlation coefficients are typical for the relationship between long-term monthly series of summer months (June and July, July and August) reflecting the period of intense and mass decrease in sea ice area in the Northern Hemisphere. Previous studies demonstrated that long-term changes in sea ice area are related to changes in the meridional gradient of insolation (MGI), which regulates the meridional heat transport in the ocean–atmosphere system. Currently, the MGI increases during the summer half-year in the hemispheres. A long-term tendency for a decrease in sea ice area during the summertime (primarily in the meridional direction) is related to an increase in the MGI. It is also known that yearly changes in sea ice area are determined by their changes during the summer half-year [*Fedorov, 2015, 2018, 2019, 2020; Fedorov et al., 2020; Fedorov and Grebennikov, 2021*]. Thus, long-term changes in sea ice area are related to long-term changes in the MGI.

Analysis of spatial relationships. Relationships between long-term series of adjacent cells of the set were analyzed to determine spatial patterns in the distribution of ice data for each month. Correlation coefficients for adjacent cells were obtained for long-term (1978–2018) series for all twelve months of the year. Then, average and maximum correlation coefficients for adjacent cells were found for each month.

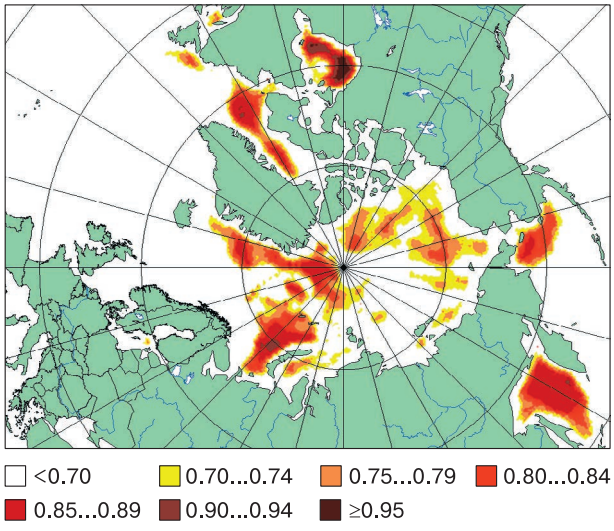

Fig. 3. Distribution of average correlation coefficient values between long-term sea ice areas in neighboring cells in March.

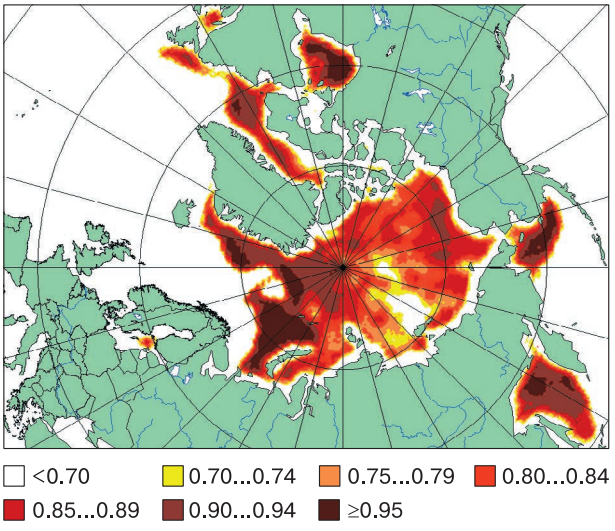

Fig. 4. Distribution of maximum correlation coefficient values between long-term sea ice areas in neighboring cells in March.

For March (the period of maximum sea ice area), the distribution of average and maximum correlation coefficients is shown in Figs. 3 and 4.

It should be noted that blank spots in a significant part of the Arctic Basin (Figs. 3 and 4) are related to limitations of the correlation analysis. The correlation coefficient is not calculated if at least one of the temporal series consists of identical variable values. Thus, for example, monthly values of sea ice area equal to 100 % of cell area were typical for a large territory of the Arctic Basin in 1978–2018.

According to average correlation coefficient values for March, the closest relationships between sea ice areas in adjacent cells of the grid are observed in the Barents and Greenland seas, in the Sea of Okhotsk and the Bering Sea, and in the Davis Strait and Hudson Bay. The maximum values of the correlation coefficient of March temporal series for adjacent cells are also localized in these areas.

The distribution of average and maximum correlation coefficients for sea ice areas in adjacent cells in September (the period of minimum sea ice area) is given in Figs. 5 and 6, respectively.

In September, the area within which a close correlation between sea ice areas in adjacent cells is observed, increases in comparison with that in March. Average and maximum correlation coefficient values also increase (Table 2).

The correlation analysis of short-range spatial relationships (between long-term sea ice area values in adjacent cells) was conducted in four possible directions. Average correlation coefficient values in all directions are presented in Table 2. The directions form naturally during calculation of correlation values of ice area in a randomly selected cell with adjacent cell data. If the selected cell is not located on the boundary of the set, correlation is possible with data on cells neighboring the selected cell from the east, west, north, south, northeast, northwest, southeast, and southwest. Thus, upon calculation of the correlation coefficient for cells of the entire data set, four directions form: north–south (N–S), east–west (E–W), southwest–northeast (SW–NE), and southeast–northwest (SE–NW).

All values of the correlation coefficient exceeding 0.5 (modulo) are statistically significant with a probability of 0.99.

On average, the number of negative values for all months is 0.271 %, positive values constitute 99.729 %. The correlation coefficient equal to zero was considered positive. As such, long-term series of monthly values in adjacent cells mainly have a positive relationship. The closeness of the correlation for average values for twelve months (an average yearly relationship) is characterized by the following correlation coefficient distribution: >0.5–92.167 %, >0.6–84.490 %, >0.7–69.354 %, >0.8–42.515 %, >0.9–12.567 %.

Maximum correlation coefficients of long-term sea ice area in adjacent cells for all twelve months of the year were also found (Table 3).

On average, over twelve months, maximum correlation coefficients values <0.0 constitute 0.217 %, and values ⩾0.0 constitute 99.783 %. The maximally close relationship averaged over twelve months (a yearly correlation) is characterized by the following distribution of the correlation coefficient: >0.5–98.270 %, >0.6–96.975 %, >0.7–94.189 %, >0.8–87.049 %, >0.9–64.010 %.

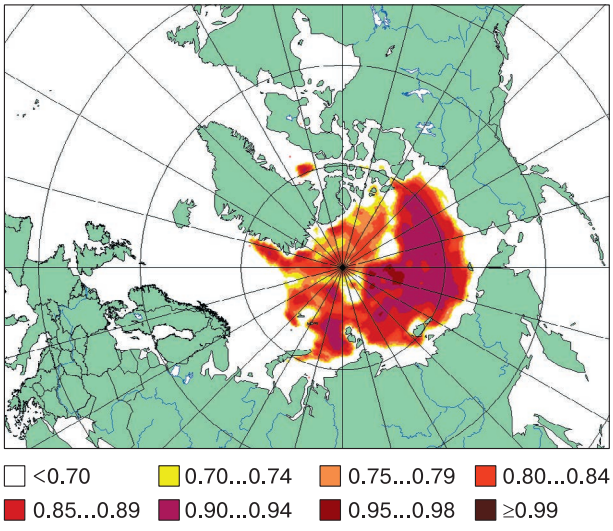

Fig. 5. Distribution of average correlation coefficient values between long-term sea ice areas in neighboring cells in September.

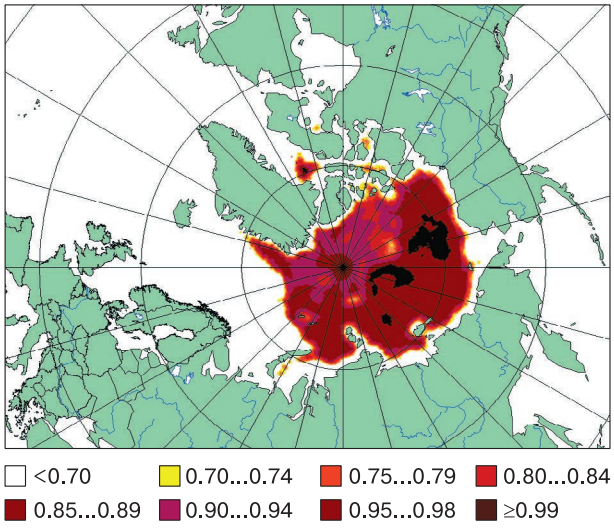

Fig. 6. Distribution of maximum correlation coefficient values between long-term sea ice areas in neighboring cells in September.

Table 2. **Distribution of average values of correlation coefficients (%) in all four correlation directions of long-term sea ice area values by months**

Correlation coefficient	January	February	March	April	May	June
< –0.9	0	0	0	0	0	0
< –0.8	0	0	0	0	0	0
< –0.7	0	0	0	0	0	0
< –0.6	0	0	0	0	0	0
< –0.5	0	0	0	0	0	0
< 0.0	0.292	0.416	0.454	0.218	0.256	0.253
⩾ 0.0	99.708	99.584	99.546	99.782	99.744	99.747
> 0.5	91.066	87.949	86.420	89.714	90.670	93.631
> 0.6	80.816	74.710	75.271	81.098	82.122	87.753
> 0.7	62.948	52.065	55.582	65.161	66.712	73.352
> 0.8	31.379	25.765	29.065	36.263	38.676	44.233
> 0.9	7.677	6.672	7.706	7.874	7.299	9.537
	July	August	September	October	November	December
< –0.9	0	0	0	0	0	0
< –0.8	0	0	0	0	0	0
< –0.7	0	0	0	0	0	0
< –0.6	0.017	0	0	0	0	0
< –0.5	0.017	0	0	0	0	0
< 0.0	0.249	0.268	0.221	0.212	0.181	0.201
⩾ 0.0	99.751	99.732	99.779	99.788	99.819	99.799
> 0.5	93.384	93.091	95.375	94.893	96.844	95.090
> 0.6	86.652	88.716	91.542	89.609	92.685	87.355
> 0.7	74.250	79.486	81.739	77.028	80.618	70.882
> 0.8	49.859	58.615	61.452	54.586	51.849	38.814
> 0.9	12.602	17.693	25.705	28.945	15.650	9.650

Table 3. **Distribution of maximum values of correlation coefficients (%) in all four correlation directions of long-term sea ice area values by months**

Correlation coefficient	January	February	March	April	May	June
< –0.9	0	0	0	0	0	0
< –0.8	0	0	0	0	0	0
< –0.7	0	0	0	0	0	0
< –0.6	0	0	0	0	0	0
< –0.5	0	0	0	0	0	0
< 0.0	0.263	0.342	0.337	0.174	0.196	0.174
⩾ 0.0	99.737	99.658	99.663	99.826	99.804	99.826
> 0.5	97.894	97.058	97.319	98.155	98.104	98.669
> 0.6	96.169	94.651	94.873	96.760	96.569	97.734
> 0.7	92.733	88.172	88.881	94.348	93.920	95.722
> 0.8	82.351	72.363	75.227	87.476	87.901	91.461
> 0.9	49.715	40.401	44.843	58.492	67.825	69.946
	July	August	September	October	November	December
< –0.9	0	0	0	0	0	0
< –0.8	0	0	0	0	0	0
< –0.7	0	0	0	0	0	0
< –0.6	0.017	0	0	0	0	0
< –0.5	0.017	0	0	0	0	0
< 0.0	0.199	0.232	0.221	0.141	0.148	0.154
⩾ 0.0	99.801	99.768	99.779	99.859	99.852	99.846
> 0.5	98.690	98.643	98.987	98.975	98.767	98.441
> 0.6	97.795	97.893	98.342	98.180	98.109	97.545
> 0.7	95.772	96.215	97.586	96.766	96.827	95.384
> 0.8	89.653	92.805	94.620	92.437	93.276	89.795
> 0.9	69.972	81.182	83.269	77.576	74.667	61.603

Table 4. **Distribution of maximum values of correlation coefficients by individual directions and months**

Correlation direction	January	February	March	April	May	June
SW–NE	6.697	7.370	6.944	5.085	4.289	3.755
N–S	6.068	7.370	6.827	4.794	3.777	2.963
SE–NW	4.708	5.423	5.054	3.225	2.950	2.725
E–W	82.527	79.837	81.175	86.895	88.984	90.558
	July	August	September	October	November	December
SW–NE	4.195	3.910	3.575	4.312	3.600	4.987
N–S	3.034	2.464	2.727	2.598	3.156	3.999
SE–NW	3.200	2.392	2.193	2.739	2.828	3.505
E–W	89.571	91.234	91.505	90.352	90.416	87.510

As noted previously, there are four possible directions of correlation. The directional distribution of maximum correlation coefficients in the months of the year is provided in Table 4.

On average, over the months of the year for the SW–NE direction, the maximum coefficient correlation values are 4.969 %; for the N–S direction, 4.254 %; for the SE–NW direction, 3.254 %; and for the E–W direction, 87.305 %. Thus, spatial anisotropy manifests itself in the ice data set correlation, which is expressed as a significant predominance of maximum correlation coefficient distribution over the E–W latitudinal direction for all months of the year.

The distribution of the maximum values of the correlation coefficient obtained for a year (by averaging monthly values) over 1-degree latitudinal zones was studied (Fig. 7). The distribution is presented as a percentage of the total number of correlation coefficient values obtained in all directions of correlation for the entire ice data set.

The predominance of the latitudinal direction in the spatial distribution of maximum correlation coefficients of long-term monthly sea ice area values in adjacent cells of the data set is noted for the entire area north of the Arctic circle. The main reason for this effect is related to the seasonal formation of ice (from northern to southern latitudes) and seasonal thawing of ice (from southern to northern latitudes) regulated by seasonal changes in insolation (or solar radiation). Long-term changes in sea ice area (related to changes in ice formation and thawing processes) are determined by changes in the meridional gradient of insolation regulated by the intensity of the meridional transport of solar radiation, the work of the "thermal machine of the first order". Changes in the meridional gradient of insolation are related to change in the Earth's axial tilt [*Fedorov, 2018, 2019, 2020; Fedorov and Grebennikov, 2021*]. Another reason for the noted effect can be the predominantly meridional drift of sea ice in the Arctic Ocean, which is determined by the character of sea currents and wind direction [*Zubov, 1938; Zakharov, 1976; Krutskikh, 1991; Frolov and Gavrilo, 1997*]. Thus, specifically meridional changes in the transport of solar radiation and predominantly the meridional direction of sea ice drift are the reasons for the observed zonal anisotropy.

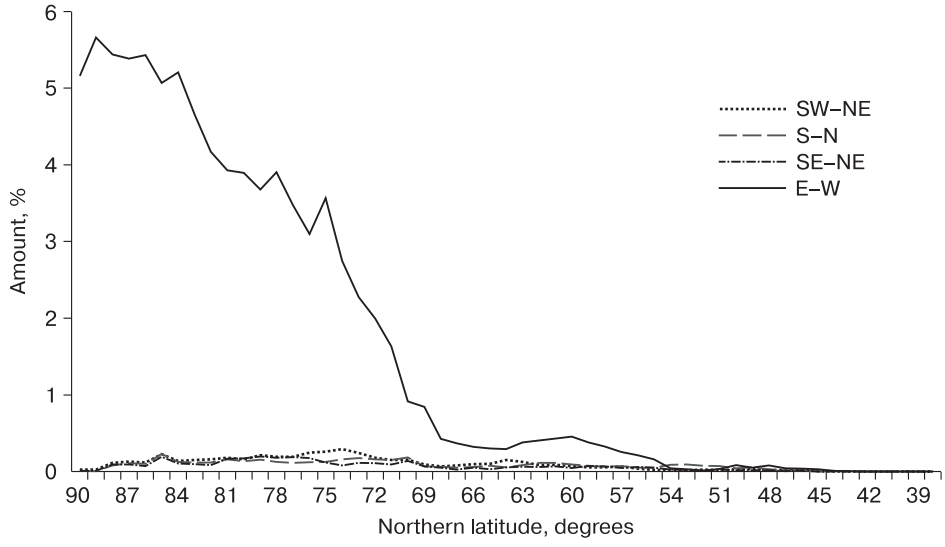

Fig. 7. Distribution of maximum correlation coefficient values in 1-degree latitudinal zones.

CONCLUSIONS

The correlation analysis of temporal relationships in the ice data set allowed us to determine that the closest relationships in long-term monthly sea ice area values are typical for June and July, July and August. Approximately half (more than 48 %) of maximum correlation coefficients between sea ice areas in the neighboring cells of the Northern Hemisphere are noted for the summer (June–August). This effect is determined by the intense and mass seasonal thawing of sea ice in the Northern Hemisphere, which is determined by the maximum influx of heat from solar radiation. Seasonal changes in sea ice area also manifest themselves in the nature of long-term changes, which are most closely related in adjacent cells in the summer. However, long-term changes are mostly determined by changes in the summer meridional gradient of insolation.

The correlation analysis of spatial relationships showed that the closest relationships for all the months of the year between long-tern monthly values are typical for the east–west latitudinal direction. More than 87 % of all maximum correlation coefficients fall here. The anisotropy is noted on the entire territory north of the Arctic Circle and is determined by the meridional direction of seasonal formation and thawing of sea ice related to seasonal meridional change in insolation (solar radiation). The seasonal nature of spatial variability in sea ice area also manifests itself in similar dynamics of long-term changes. Long-term changes in sea ice area are determined by long-term changes in the meridional gradient of insolation which regulates the intensity of meridional transport of solar radiation from the equatorial region to polar regions. Another reason for spatial anisotropy is possibly a predominantly meridional drift direction in the Arctic Ocean.

Regions with high and low levels of short-term spatial and temporal relationships in the dynamics of sea ice areas in the Northern Hemisphere have been identified. The obtained autocorrelation characteristics can be considered for interpolation and extrapolation of sea ice area data and, thus, contribute to refining ice data sets. The obtained results – regional specificity of short-range spatial and temporal relationships – can also be taken into consideration for statistical and physicomathematical modeling of the dynamics of sea ice areas in the Northern Hemisphere.

Acknowledgments. *This study has been performed within the framework of budgetary themes "Evolution, the modern state and prognosis of the development of the coastal zone of the Russian Arctic" (121051100167-1), "Dangers and risks of natural processes and phenomena" (121051300175-4), and "Evolution of the cryosphere during climate change and anthropogenic influence" (121051100164-0).*

References

Fedorov, V.M., 2015. Trends of the changes in sea ice extent in the Northern Hemisphere and their causes. Earth's Cryosphere XIX (3), 46–57.

Fedorov, V.M., 2018. Earth's Insolation and Recent Climate Changes. Fizmatlit, Moscow, 232 p. (in Russian).

Fedorov, V.M. 2019. The problem of meridional heat transport in the astronomical climate theory. Izv. Atmos. Ocean. Phys. 55, 1572–1583.

Fedorov, V.M., 2020. Evolution of the modern global climate of the Earth and its possible causes. GeoRisk XIV (4), 16–29, doi: 10.25296/1997-8669-2020-14-4-16-29

Fedorov, V.M., Grebennikov, P.B., Frolov, D.M., 2020. Analysis of responses in the dynamics of sea ice area of individual regions of the Arctic for changes in insolation. Arktika i Antarktika, No. 2, 17–33, doi: 10.7256/2453-8922.2020.2.31875

Fedorov, V.M., Grebennikov, P.B., 2021. Implications of changes in insolation characteristics for long-term sea ice extent dynamics in the Northern Hemisphere. Earth's Cryosphere XXV (2), 35–43.

Frolov, I.E., Gavrilo, V.P. (Eds.), 1997. Sea Ice. Gidrometeoizdat, St. Petersburg, 402 p. (in Russian).

Kondratiev, K.Ya., 1980. Radiation Factors of Modern Changes in Global Climate. Gidrometeoizdat, Leningrad, 279 p. (in Russian).

Kondratiev, K.Ya., 1992. Global Climate. Nauka, St. Petersburg, 359 p. (in Russian).

Krutskikh, B.A. (Ed.), 1991. Climate Regime of the Arctic at the Turn of the 20th and 21st Centuries. Gidrometeoizdat, Leningrad, 200 p. (in Russian).

Monin, A.S., 1982. Introduction to the Theory of Climate. Gidrometeoizdat, Leningrad, 246 p. (in Russian).

Rayner, N.A., Parker, D.E., Horton, E.B. et al., 2003. Global analyses of sea surface temperature, sea ice, and night marine air temperature since the late nineteenth century. J. Geophys. Res. **108**, No. D14, 4407, doi: 10.1029/2002JD002670

Shuleikin, V.V., 1953. Sea Physics. Izd. Akad. Nauk SSSR, Moscow, 990 p. (in Russian).

URL: http://www.metoffice.gov.uk/hadobs/hadisst/data/download.html (last visited: February 25, 2021).

Zakharov, V.F., 1976. Cooling of the Arctic and the ice cover of the Arctic seas. Tr. AANII, vol. 337, p. 96 (in Russian).

Zakharov, V.F., Malinin, V.N., 2000. Sea Ice and Climate. Gidrometeoizdat, St. Petersburg, 92 p. (in Russian).

Zaks, L., 1976. Statistical Evaluation. Statistika, Moscow, 598 p. (in Russian).

Zubakin, G.K. (Ed.), 2006. Ice Formations in the Western Arctic Seas. AARI, St. Petersburg, 272 p. (in Russian).

Zubov, N.N., 1938. Sea Water and Sea Ice. Gidrometeoizdat, Moscow, 454 p. (in Russian).

Received February 26, 2021
Revised December 27, 2021
Accepted January 4, 2022

Translated by M.A. Korkka